

**Resonant x-ray scattering from LaSr<sub>2</sub>Mn<sub>2</sub>O<sub>7</sub> at the Mn K edge**S. Di Matteo,<sup>1</sup> Tapan Chatterji,<sup>2,3</sup> Y. Joly,<sup>4</sup> A. Stunault,<sup>1</sup> J. A. Paixao,<sup>5</sup> R. Suryanarayanan,<sup>6</sup> G. Dhallene,<sup>6</sup> and A. Revcolevschi<sup>6</sup><sup>1</sup>*INFN, UdR Roma III and INFN, Laboratori Nazionali di Frascati, via Enrico Fermi 40, I-00044 Frascati (Roma), Italy*<sup>2</sup>*Institut Laue-Langevin, BP 156, F-38042 Grenoble Cedex 9, France*<sup>3</sup>*Max-Planck-Institut für Physik Komplexer Systeme, Dresden, Germany*<sup>4</sup>*Laboratoire de Cristallographie, CNRS, BP166, F-38042 Grenoble Cedex 9, France*<sup>5</sup>*European Synchrotron Facility, BP 220, F-38043 Grenoble Cedex, France*<sup>6</sup>*Laboratoire de Physico-Chimie de l'Etat Solide, Université Paris-Sud, F-91405 Orsay, France*

(Received 12 November 2002; revised manuscript received 21 March 2003; published 23 July 2003)

We have investigated Mn *K* edge resonant scattering from a single crystal of the bilayered manganite LaSr<sub>2</sub>Mn<sub>2</sub>O<sub>7</sub> in the charge/orbital ordered state ( $T=170$  K). A strong intensity enhancement of the tetragonal superlattice reflection  $(-\frac{1}{4}, \frac{1}{4}, 10)$  has been observed as the x-ray energy is tuned to the Mn *K* edge. In recent years a strong controversy arose regarding the nature of these kinds of superlattice reflections, i.e., whether their origin is due to Jahn-Teller distortion, orbital ordering, or both. We have thus performed realistic calculations to simulate the resonant signal, based on multiple-scattering theory and the finite difference method. We have found that Jahn-Teller distortion alone correctly describes the main features of the experimental data, the orbital ordering contribution being one order-of-magnitude smaller in amplitude.

DOI: 10.1103/PhysRevB.68.024414

PACS number(s): 78.70.Ck, 61.10.Dp, 75.25.+z, 75.30.Ds

**I. INTRODUCTION**

Strongly correlated electron systems such as transition-metal oxides have recently become the subject of numerous experimental and theoretical studies after the discovery of a variety of different physical phenomena and a diversity of ordered phases.<sup>1</sup> In particular, the interplay among spin, charge, orbital, and lattice degrees of freedom in manganites has attracted considerable attention because of the colossal magnetoresistance behavior of these compounds. A powerful experimental technique to analyze structural and electronic ordered phases is elastic resonant x-ray scattering (RXS), since the resonant scattering process depends on the anisotropy of the empty electronic levels as determined not only by the orbital filling on the resonant atom, but also by the geometrical distribution of its neighbors.

With this method Murakami *et al.*<sup>2,3</sup> observed a strong intensity enhancement for some Bragg-forbidden reflections in La<sub>0.5</sub>Sr<sub>1.5</sub>MnO<sub>4</sub> and LaMnO<sub>3</sub>. From the azimuthal angle dependence they concluded they had observed directly the orbital ordering (OO) in these compounds. These claims have been later supported by the MnO<sub>6</sub> cluster calculations of Ishihara and Maekawa,<sup>4</sup> who found that the orbital dependence of the  $3d-4p$  Coulomb interaction is essential to the anisotropy of the scattering factor near the Mn *K* edge. Nonetheless, they have been contested by several other authors.<sup>5-7</sup> Elfimov *et al.*,<sup>5</sup> on the basis of their local spin-density approximation +  $U$  calculations, showed that the x-ray resonance scattering at the Mn *K* edge could be sensitive to orbital ordering but in a lower-energy range than experimentally observed and also that multielectronic effects are negligible. Similarly, Benfatto *et al.*<sup>6</sup> concluded, from their calculations based on multiple-scattering theory and the finite difference method, that the contribution of Jahn-Teller distortion (JTD) to the Bragg-forbidden resonant x-ray signal in LaMnO<sub>3</sub> at Mn *K* edge is at least two orders-of-magnitude

greater than the one due to orbital ordering. This same conclusion has been confirmed by Takahashi *et al.*<sup>7</sup> on the basis of their local-density band-structure calculations. In spite of all this, in recent review papers Murakami, Ishihara, and Maekawa<sup>8</sup> and Ishihara and Maekawa<sup>9</sup> have reiterated their claims of direct observation of orbital order by RXS. Also Inami *et al.*<sup>10</sup> reported their experiment of resonant inelastic x-ray scattering (RIXS) as direct observation of orbital excitations. There have been claims<sup>9</sup> that RXS and RIXS would open up the field of orbital physics in a similar way as spin physics had been probed by neutron scattering during the last half century. In light of the latter considerations, we believe that it is important to analyze all the cases that led to such claims. Those concerning LaMnO<sub>3</sub> and La<sub>0.5</sub>Sr<sub>1.5</sub>MnO<sub>4</sub> have already been critically reviewed in Refs. 5-7.

The main point of the present paper is to show that also the case of the bilayered manganite LaSr<sub>2</sub>Mn<sub>2</sub>O<sub>7</sub>, treated by Wakabayashi *et al.*<sup>11</sup> and Ishihara and Maekawa<sup>12</sup> as direct evidence for orbital ordering, can be adequately described by the JTD of MnO<sub>6</sub> octahedra alone. We measured some Bragg-forbidden reflections where we found a strong resonant intensity enhancement and analyzed them by *ab initio* calculations based on multiple scattering and the finite difference method. Our results show that the contribution of orbital order to RXS intensity is only about one percent of the JTD one, i.e., we are in favor for rejecting the idea that OO can be considered mainly responsible of the RXS signal at the *K* edge. We believe it is worthwhile to stress this result because, in spite of the previous similar ones obtained in Refs. 5-7, the theoretical considerations performed in Refs. 11 and 12 about the bilayered compound LaSr<sub>2</sub>Mn<sub>2</sub>O<sub>7</sub> again do not take JTD into account. Yet, this does not mean that the OO contribution cannot be detected, for example, at other edges, as very well described by Castleton and Altarelli<sup>13</sup> for the case of  $L_{2,3}$  edges.

## II. DESCRIPTION OF THE COMPOUND AND EXPERIMENTAL SETUP

We focused on the bilayered manganites  $\text{La}_{2-2x}\text{Sr}_{1+2x}\text{Mn}_2\text{O}_7$  that have become the subject of intense investigation after the recent discovery of colossal magnetoresistance behavior.<sup>14,15</sup> Because of the reduced dimensionality the physical properties of these bilayered manganites are different from those of three-dimensional manganites.<sup>16</sup> For example, the magnetoresistance is greatly enhanced in the bilayered manganite, for  $x=0.4$ , but only at the cost of a reduced ferromagnetic transition temperature. Since the 50% hole-doped ( $x=\frac{1}{2}$ )  $\text{LaSr}_2\text{Mn}_2\text{O}_7$  consists of formally equal amounts of  $\text{Mn}^{3+}$  and  $\text{Mn}^{4+}$  ions, one expects, in analogy with three-dimensional manganites, that charge ordering and ordering of the orbitals are associated.<sup>17,18</sup> A neutron-diffraction and high-energy x-ray-diffraction investigation of the charge-orbital ordering in  $\text{LaSr}_2\text{Mn}_2\text{O}_7$  has been previously reported:<sup>19</sup> Below  $T_{CO}\approx 210$  K,  $\text{LaSr}_2\text{Mn}_2\text{O}_7$  shows superlattice reflections corresponding to an orthorhombic distortion of the high-temperature tetragonal lattice  $I4/mmm$  (number 139 of Ref. 20), with a quadrupling of the unit volume. The onset of a distorted phase at  $T_{CO}\approx 210$  K had been found also by Kubota *et al.*<sup>21</sup> The bottom panel of Fig. 1 shows the  $\text{MnO}_2$ -plane projection of both cells. The Mn ions in the orthorhombic phase occupy two inequivalent crystallographic positions of the space group  $Bbmm$  [number 63 of Ref. 20 rotated by  $120^\circ$  along the (111) direction], as determined in Refs. 19 and 22. Specifically, we can identify a  $\text{Mn}_1$ , with Wyckoff symmetry  $8e$ , with a formal state of oxidation  $3+$  and a  $\text{Mn}_2$ , with Wyckoff symmetry  $8g$ , with a formal state of oxidation  $4+$ . The top part of Fig. 1 shows the projection of the charge-orbital ordered structure of  $\text{LaSr}_2\text{Mn}_2\text{O}_7$  perpendicular to the  $c$  axis. The arrows show the displacement of the atoms in the charge-orbital ordered state with respect to the tetragonal phase. The two crystallographic positions which are associated with  $\text{Mn}^{3+}$  and  $\text{Mn}^{4+}$  ions correspond to the light gray and the dark gray squares, respectively. The Mn-O bond distances are nearly equal for the  $\text{Mn}^{4+}$  ions whereas the Jahn-Teller  $\text{Mn}^{3+}$  ions have different bond distances, as shown in the light gray squares. The bottom of Fig. 1 shows the schematic representation of the proposed orbital ordering in Ref. 11. Note that the longer  $\text{Mn}^{3+}$ -O bond distance corresponds to the direction along which  $d_{3\eta^2-r^2}$  orbitals are extended (the quantization axis  $\eta$  is chosen according to Ref. 2).

RXS experiments were performed on the beam line ID20 of the European Synchrotron Radiation Facility at Grenoble. The beam line was equipped with a four-circle diffractometer with a vertical scattering plane. A plate-shaped single crystal of linear dimensions  $4 \times 2 \times 0.5$  mm<sup>3</sup> was mounted on a copper sample holder with the [001] crystallographic axis of the crystal (tetragonal  $I4/mmm$  indexing) perpendicular to the plane of the plate. A closed-cycle He Displex cryostat with Be domes was used to cool the crystal. The temperature of the sample was kept at  $T=170$  K at which the superlattice reflections have highest intensities. The detector arm was equipped with a polarization analyzer Cu (220) single crystal. Among the measured reflections, here we focus only on

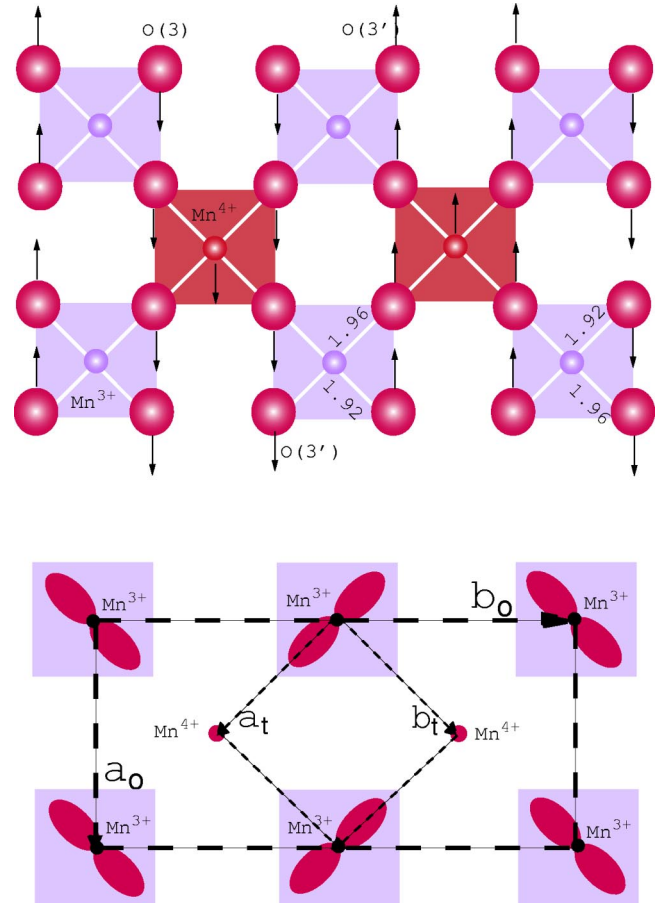


FIG. 1. (top) Projection in the  $\text{MnO}_2$  plane of the crystal structure of the charge-orbital ordered phase of  $\text{LaSr}_2\text{Mn}_2\text{O}_7$  at  $T = 170$  K. (bottom) Schematic representation of the proposed orbital ordering. We also show the in-plane projections of the high-temperature tetragonal cell (short-dashed lines) and low-temperature orthorhombic cell (long-dashed lines).

the  $(-\frac{1}{4}, \frac{1}{4}, 10)$  tetragonal superlattice reflection since it is sufficient for our purposes.

The mechanism of RXS is the following: the incoming photon is virtually absorbed and a core electron is promoted to an empty state leaving a core hole behind. Then the excited electron decays back to the same core hole emitting an outgoing photon with the same energy as the incoming one and, eventually, a different wave vector and polarization. Since the excited electron is sensitive, in principle, to any anisotropy around the absorbing ion (charge, orbital, lattice, magnetic), it turns out that the atomic scattering factor  $F_{\text{Mn}}$  has a tensorial character. Moreover, it strongly depends on the photon energy in the anomalous dispersion region. In our case we deal with a transition from a  $1s$ -core state to a  $4p$  band and for this reason we can consider the scattering factor in the dipole approximation. In this case,  $F_{\text{Mn}}$  can be written as

$$F_{\text{Mn}} \equiv \sum_n \frac{\langle \Psi_0 | \vec{\epsilon}^2 \cdot \vec{r} | \Psi_n \rangle \langle \Psi_n | \vec{\epsilon}^i \cdot \vec{r} | \Psi_0 \rangle}{\hbar \omega - (E_n - E_0) - i\Gamma}, \quad (1)$$

TABLE I. Fractional coordinates in terms of  $a_o$ ,  $b_o$ , and  $c_o$ .

| i | $\text{Mn}^{3+}(8e)$ | $\text{Mn}^{4+}(8g)$  |
|---|----------------------|-----------------------|
| 1 | 0.0, 0.0, 0.09696    | 0.5065, 0.25, 0.09696 |
| 2 | 0.0, 0.0, 0.90304    | 0.5065, 0.25, 0.90304 |
| 3 | 0.5, 0.0, 0.59696    | 0.0065, 0.25, 0.59696 |
| 4 | 0.5, 0.0, 0.40304    | 0.0065, 0.25, 0.40304 |
| 5 | 0.0, 0.5, 0.09696    | 0.4935, 0.75, 0.09696 |
| 6 | 0.0, 0.5, 0.90304    | 0.4935, 0.75, 0.90304 |
| 7 | 0.5, 0.5, 0.59696    | 0.9935, 0.75, 0.59696 |
| 8 | 0.5, 0.5, 0.40304    | 0.9935, 0.75, 0.40304 |

where  $\hbar\omega$  is the energy of the incoming and outgoing photons,  $\Psi_0$  ( $\Psi_n$ ) is the ground (excited) state of the system,  $\Gamma$  represents the broadening of the resonance, and  $\vec{\epsilon}^o$  ( $\vec{\epsilon}^i$ ) is the outgoing (incoming) polarization. We neglected the complex conjugation for  $\vec{\epsilon}^o$  because we are dealing with real polarizations. The crystal scattering amplitude is then the sum, over all the Mn ions of the unit cell, of each atomic scattering factor, weighted as usual by the appropriate Bragg factor. For forbidden reflections, the sum of the Bragg factors is zero so that the usually dominating scalar Thomson factor vanishes: only the anomalous behavior is then present.

Consider the specific case of the Bragg-forbidden reflection  $(-\frac{1}{4}, \frac{1}{4}, 10)$ . For convenience we can write it in orthorhombic units as  $(0, 1, 10)_o$ . In this way the evaluation of the structure factor is easier, as well as the identification of Bragg planes in the reference frame of Fig. 1. In the orthorhombic unit cell there are 8 f.u. with 16 Mn ions so that the structure factor can be written as

$$A = \sum_{i=1}^{16} e^{i\vec{Q}\cdot\vec{R}_i} F_{\text{Mn}}^i, \quad (2)$$

where  $\vec{Q}$  is the Bragg vector,  $(0, 1, 10)_o$  in our case, and  $\vec{R}_i$  is the position of the  $\text{Mn}^{3+}$  and  $\text{Mn}^{4+}$  ions given in Table I in terms of the orthorhombic unit axes. Each element  $F_{\text{Mn}}^i$  is a tensor, expressed by Eq. (1). Referring to the following Table I for the positions of manganese ions, it is clear that for each  $(x, y, z)$  there is another ion in the position  $(\bar{x}, y + 1/2, z)$ , for each group 8e and 8g.

Since the specific reflection  $(0, 1, 10)_o$  does not depend on the first position coordinate, it becomes possible to write Eq. (2) in the form

$$A = \sum_{i=1}^4 e^{i\vec{q}\cdot\vec{R}_i} [(F_{\text{Mn}^{4+}}^{i+4} - F_{\text{Mn}^{4+}}^{i+4}) + (F_{\text{Mn}^{3+}}^i - F_{\text{Mn}^{3+}}^{i+4})]. \quad (3)$$

Thus, for each group of eight, the total anomalous scattering factor depends on the difference between the local amplitudes of the two Mn ions connected by the  $(0, \frac{1}{2}, 0)_o$  translation in the orthorhombic unit.  $\text{Mn}^{4+}$  ions connected by the  $(0, \frac{1}{2}, 0)_o$  translation have the same local charge distribution: the symmetry operation that connects them is just identity. Thus, their contribution to the scattering amplitude is zero ( $F_{\text{Mn}^{4+}}^i = F_{\text{Mn}^{4+}}^{i+4}$ ): only  $\text{Mn}^{3+}$  ions contribute to the

scattering amplitude, since the two  $\text{Mn}^{3+}$  ions connected by the  $(0, \frac{1}{2}, 0)_o$  translation have different local symmetries. In order to write their contribution explicitly, we make use of the following relations, describing the symmetry operations that connect the 8e sites to one another (from now on we remove the  $\text{Mn}^{3+}$  index):

$$F_2 = \hat{I}F_1, \quad F_5 = \hat{\sigma}_{x(y)}F_1, \quad F_6 = \hat{I}\hat{\sigma}_{x(y)}F_1, \\ F_3 = F_1, \quad F_4 = F_2, \quad F_7 = F_5, \quad F_8 = F_6,$$

where  $F_i$  indicates the  $i$ th ion,  $\hat{I}$  is the inversion, and  $\hat{\sigma}_{x(y)}$  the mirror operator with respect to the  $x \equiv a_o$  ( $y \equiv b_o$ ) plane. These relations can be derived from Ref. 20, number 63 (rotated, as mentioned above). In this way Eq. (3) can be rewritten as

$$A = e^{2\pi iz_0}(F_1 - F_5 + F_3 - F_7) + e^{-2\pi iz_0}(F_2 - F_6 + F_4 - F_8) \\ = 2[e^{2\pi iz_0} + \hat{I}e^{-2\pi iz_0}][1 - \hat{\sigma}_{x(y)}]F_1, \quad (4)$$

where  $z_0 = 0.09696$ .

The atomic scattering factor is scalar with respect to rotoinversion operations: it can be written as the scalar product between two tensors, one representing the properties of the system, the other the properties of the light.<sup>23</sup> When we write Eq. (4) the inversion or mirror operators are intended to act only on one of the previous two tensors, leaving the other unaltered. Since we are dealing with nonmagnetic properties in the dipolar approximation, the two tensors can have only rank 0 or 2. The scalar is forbidden because of the mirror symmetry of Eq. (4) (thus recovering the extinction rule for the usual Thomson scattering). Of the five components of the rank-2 tensor, only the symmetric combination  $F_{xy} + F_{yx}$  survives, since it changes sign under the action of both mirror symmetries  $[\hat{\sigma}_{x(y)}]$ . On the contrary, all the other four components ( $F_{xz} + F_{zx}$ ,  $F_{yz} + F_{zy}$ ,  $F_{x^2 - y^2}$ , and  $F_{3z^2 - r^2}$ ) are invariant with respect to at least one of the two mirror symmetries  $[\hat{\sigma}_{x(y)}]$  and their contribution in Eq. (4) vanishes. This tensor is coupled to the similar linear combination  $\epsilon_x^o \epsilon_y^i + \epsilon_y^o \epsilon_x^i$  of the polarization vectors; this analysis is used in the following section.

### III. RESULTS AND DISCUSSION

The intensity of the  $(-\frac{1}{4}, \frac{1}{4}, 10)$  reflection was measured as a function of energy, close to the Mn  $K$  absorption edge in both  $\sigma$ - $\sigma$  and  $\sigma$ - $\pi$  channels (Fig. 2). Strong resonances have been observed in both cases at about  $E = 6553$  eV.

Our method of calculation (FDMNES package<sup>24</sup>) uses optionally the finite difference method (FDM) or the multiple-scattering theory<sup>25</sup> (MST) to solve the Schrödinger equation. The FDM formalism applied to x-ray-absorption spectroscopy calculations was already reported.<sup>26</sup> We just recall that the FDM is based on the elaboration of a three-dimensional grid in the volume of interest, and a discrete form of the Schrödinger equation is given on the node points of this grid. The input data are the electronic charge distributions of the ions in the cluster, whose orientation can be chosen at will.

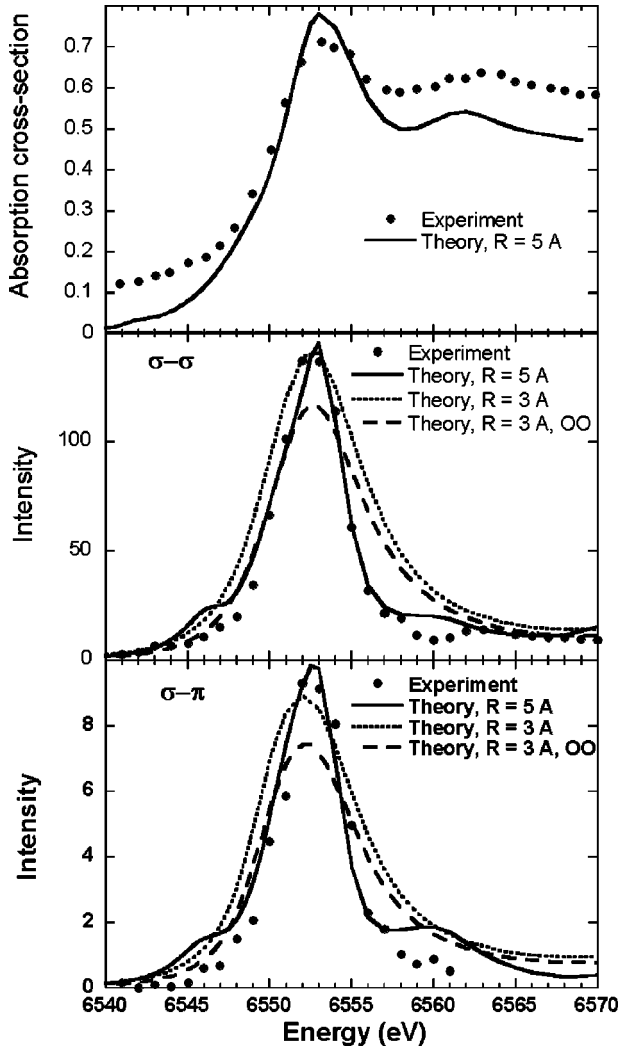


FIG. 2. (a) Energy dependence (experiment and theory) of the fluorescence intensity from the  $\text{LaSr}_2\text{Mn}_2\text{O}_7$  single crystal at  $T = 170$  K close to the Mn  $K$  absorption edge. (b) Energy dependence (experiment and theory) of the superlattice reflection  $(-\frac{1}{4}, \frac{1}{4}, 10)$  in the  $\sigma\text{-}\sigma$  channel at  $T = 170$  K. (c) Same as (b) in the  $\sigma\text{-}\pi$  channel.  $R$  is the radius of the cluster used in the calculations.

Solving Poisson's equation, the Coulomb potential is obtained, and the exchange-correlation term is calculated in the Hedin-Lundqvist approximation.<sup>27</sup> In this way it is possible to use an arbitrary shape for the potential and thus avoid the muffin-tin approximation used in our MST calculations. With this latter option, in fact, the potential is spherically averaged around each atom up to a specific radius. In the interstitial area, between the atomic spheres, the potential is constant. This approximation forbids the OO analysis and makes necessary the FDM approach. Nevertheless this latter is highly CPU consuming and we can use it only for a rather small cluster size. So calculations are performed in two steps, first with a small cluster radius  $R$  to look at the relative influence of OO and JTD, using both FDM and MST modes, and later in the MST mode, up to a higher radius sufficient to get good experiment-theory agreement.

We used, as input data, the crystallographic positions ob-

tained from the neutron refinement<sup>28</sup> (quantitatively similar results are obtained using those of Ref. 22). Two of the three calculations shown in Fig. 2, those with a 3-Å cluster radius, are performed in the FDM non-muffin-tin approach. In all cases the use of the real, orthorhombic crystal structure automatically introduces the effect of the lattice distortion (i.e., JTD) in the calculated potential. The plot labeled "OO" includes also the orbital anisotropy. In this latter case the potential is calculated with a nonspherical occupancy of the Mn  $d$  orbitals. Following Murakami *et al.*<sup>2</sup> the ordering occurs with a  $d_{\eta^2}$ -type orbital, the local  $\eta$  axis being perpendicular to the  $c_o$  axis and alternatively at  $\pm 45^\circ$  of the  $a_o$  axis (see Fig. 1). As shown in Fig. 2, the main feature of the anomalous signal is already present in the spectra with the 3-Å cluster radius and does not need OO. The inclusion of the OO decreases the signal, as a consequence of a destructive interference between this effect with JTD. The reduction of the global intensity is about 20%: the calculated amplitude ratio between the "pure" OO signal and the "pure" JTD signal is found to be 1 to 10. This is the same ratio already found in Ref. 6 for  $\text{LaMnO}_3$ . Note that this similarity with the case of  $\text{LaMnO}_3$  could be somehow expected since the resonant signal is essentially due to the resonant ion together with its surroundings, and these features are similar in  $\text{LaMnO}_3$  and in  $\text{LaSr}_2\text{Mn}_2\text{O}_7$ .

When we increase the cluster size, up to 5 Å, using the MST mode calculation, the agreement with experimental data is improved for both the x-ray-absorption near-edge structure spectrum and the anomalous signal. At 5 Å the second neighboring Mn atoms are included in the cluster, and, as a consequence, the secondary peak at 6561 eV appears in the absorption spectra together with the corresponding features in the anomalous signal, in both  $\sigma\sigma$  and  $\sigma\pi$  channels (see Fig. 2, "Theory,  $R = 5$  Å"). The quality of the final agreement including the relative amplitude between the main peaks of the spectra in  $\sigma\sigma$  and  $\sigma\pi$  channels (ratio of about 14 at the maximum energy) is further proof that JTD alone is sufficient to describe the main features of the experimental data.

The symmetry considerations sketched at the end of the previous section allow us to explain also the angular dependence of the experimental signal. We report it here for completeness, even if it should be clear that, as far as the fact that JTD and OO have the same symmetry around the  $\text{Mn}^{3+}$  resonant ion, the azimuthal scan cannot discriminate between them. (This is clear also from the model given in Ref. 3.) Because of its polarization dependence, the signal is proportional to the expectation value over the final scattering states<sup>29</sup> of the operator  $\hat{L}_x\hat{L}_y + \hat{L}_y\hat{L}_x$ , i.e., a quadrupolar operator that has fourfold symmetry around the  $z$  axis, even if the system itself, in the orthorhombic phase, no longer has such symmetry around each Mn ion. The fourfold symmetry of this operator is modulated by the polarization prefactor  $\epsilon_x^o\epsilon_y^i + \epsilon_y^o\epsilon_x^i$ . For the  $\sigma\sigma$  channel,  $\vec{\epsilon} = \vec{\epsilon}^o$ , so that also the polarization prefactor has fourfold symmetry. The minima are reached along the orthorhombic axes  $a_o$  and  $b_o$  and the maxima along the diagonals, as confirmed by a numerical simulation. In the  $\sigma\pi$  channel this is not true: the fourfold

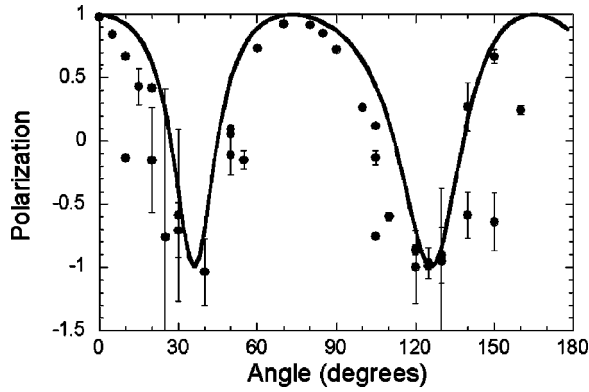


FIG. 3. Azimuthal angular dependence (experiment and theory) of the polarization of the  $(-\frac{1}{4}, \frac{1}{4}, 10)$  reflection of  $\text{LaSr}_2\text{Mn}_2\text{O}_7$  at the maximum energy  $E = 6553$  eV.

periodicity is modulated by the projection of the  $\epsilon^\pi$  component on the  $xy$  plane that has no symmetry at all, because of the canted direction of the  $\vec{Q}$  vector with respect to the  $z$  axis. All this explains why the angular fourfold behavior experimentally found in the polarization  $P$  is only approximate. The polarization is defined by

$$P = \frac{I_{\sigma\sigma} - I_{\sigma\pi}}{I_{\sigma\sigma} + I_{\sigma\pi}}. \quad (5)$$

We have chosen to plot the polarization instead of the separate azimuthal scans in the  $\sigma\sigma$  and  $\sigma\pi$  channels, because our sample was not homogeneous and in the azimuthal rotation we could not prevent the beam from focusing on different regions.  $P$  turns out to be more reliable for comparisons because it is normalized.

Figure 3 describes  $P$  as a function of the azimuthal angle  $\psi$  around the scattering vector at the maximum energy  $E = 6553$  eV. The experimental data are in good agreement with the theoretical simulations performed in the MST (cluster radius  $5 \text{ \AA}$ ), with JTD alone.

Before concluding, we would like to stress the validity of our method of calculations, through independent qualitative

considerations. The FDM approach (as well as the MST) is a single particle approach. As such it is expected to fail only when electronic correlations overwhelm band effects. This latter case would be very unusual for a  $4p$ , extended Mn band. In fact, borrowing some results from Ref. 6, we are able to list some very simple arguments that independently establish an order of magnitude of the effects and substantiate our conclusions:

(i) From band calculations, the splitting between  $x$  and  $y$  components at the  $4p$  energy level due to Mn-O bond distortion is about 1.6 eV.

(ii) The corresponding splitting due to  $3d-4p$  Coulomb repulsion is  $\frac{6}{35}F^2 = 0.4$  eV, where the  $F^2$  Slater parameter is evaluated in the atomic approximation as 2.5 eV (by means of Cowan's program).

(iii) Following the model in Ref. 3, the signal is proportional to the square of such a splitting: this simple consideration already gives a factor of 16 in intensity in favor of the JTD. The effect is further increased by the reduction of  $F^2$  due to band effects.

(iv) In Ref. 4, citation number 20, in order to explain the signal as due to OO, it is assumed that a value for  $F^2 \equiv 35F_2 = 10.5$  eV, more than four times its atomic value, which is highly unphysical.

In conclusion, we performed a RXS experiment on  $\text{LaSr}_2\text{Mn}_2\text{O}_7$  and analyzed it with the help of *ab initio* calculations. The anomalous signal of the forbidden reflections is perfectly understood both qualitatively and quantitatively simply invoking the JTD. Such a signal comes only from the ordered geometrical distortions around the resonant ions. Thus, orbital ordering should be less emphasized to explain the RXS Mn  $K$  edge when it is associated with Jahn-Teller displacements of the same symmetry, since this latter effect is definitively larger.

#### ACKNOWLEDGMENT

We would like to acknowledge C.R. Natoli for a careful reading of the manuscript.

<sup>1</sup>M. Imada, A. Fujimori, and Y. Tokura, *Rev. Mod. Phys.* **70**, 1039 (1998).

<sup>2</sup>Y. Murakami, H. Kawada, H. Kawata, M. Tanaka, T. Arima, Y. Moritomo, and Y. Tokura, *Phys. Rev. Lett.* **80**, 1932 (1998).

<sup>3</sup>Y. Murakami, J.P. Hill, D. Gibbs, M. Blume, I. Koyama, M. Tanaka, H. Kawata, T. Arima, Y. Tokura, K. Hirota, and Y. Endoh, *Phys. Rev. Lett.* **81**, 582 (1998).

<sup>4</sup>S. Ishihara and S. Maekawa, *Phys. Rev. Lett.* **80**, 3799 (1998).

<sup>5</sup>I.S. Elfimov, V.I. Anisimov, and G.A. Sawatzky, *Phys. Rev. Lett.* **82**, 4264 (1999).

<sup>6</sup>M. Benfatto, Y. Joly, and C.R. Natoli, *Phys. Rev. Lett.* **83**, 636 (1999).

<sup>7</sup>M. Takahashi, J. Igarashi, and P. Fulde, *J. Phys. Soc. Jpn.* **68**, 2530 (1999).

<sup>8</sup>Y. Murakami, S. Ishihara, and S. Maekawa, in *Colossal Magnetoresistive Manganites*, edited by T. Chatterji (Kluwer Academic, New York, 2002).

<sup>9</sup>S. Ishihara and S. Maekawa, *Rep. Prog. Phys.* **65**, 561 (2002).

<sup>10</sup>T. Inami, T. Fukuda, J. Mizuki, S. Ishihara, H. Kondo, H. Nakao, T. Matsumura, K. Hirota, Y. Murakami, S. Maekawa, and Y. Endoh, *Phys. Rev. B* **67**, 045108 (2003).

<sup>11</sup>Y. Wakabayashi, Y. Murakami, I. Koyama, T. Kimura, Y. Tokura, Y. Moritomo, K. Hirota, and Y. Endoh, *J. Phys. Soc. Jpn.* **69**, 2731 (2000).

<sup>12</sup>S. Ishihara and S. Maekawa, *Phys. Rev. B* **62**, 5690 (2000).

<sup>13</sup>C.W.M. Castleton and M. Altarelli, *Phys. Rev. B* **62**, 1033 (2000).

<sup>14</sup>Y. Moritomo, A. Asamitsu, H. Kuwahara, and Y. Tokura, *Nature (London)* **380**, 141 (1996).

- <sup>15</sup>D.N. Argyriou, J.F. Mitchell, C.D. Potter, S.D. Bader, R. Kleb, and J.D. Jorgensen, *Phys. Rev. B* **55**, R11965 (1997).
- <sup>16</sup>*Colossal Magnetoresistive Oxides*, edited by Y. Tokura (Gordon and Breach, New York, 2000).
- <sup>17</sup>J.Q. Li, Y. Matsui, T. Kimura, and Y. Tokura, *Phys. Rev. B* **57**, R3205 (1998).
- <sup>18</sup>T. Kimura, R. Kumai, Y. Tokura, J.Q. Li, and Y. Matsui, *Phys. Rev. B* **58**, 11 081 (1998).
- <sup>19</sup>T. Chatterji, G.J. McIntyre, W. Caliebe, R. Suryanarayanan, G. Dhalenne, and A. Revcolevschi, *Phys. Rev. B* **61**, 570 (2000).
- <sup>20</sup>*International Tables for Crystallography*, 5th ed., edited by Theo Hahn (Kluwer, Dordrecht, 2002)
- <sup>21</sup>M. Kubota, H. Yoshizawa, Y. Moritomo, H. Fujioka, K. Hirota, and Y. Endoh, *J. Phys. Soc. Jpn.* **68**, 2202 (1999); **69**, 1606 (2000).
- <sup>22</sup>D.N. Argyriou, H.N. Bordallo, B.J. Campbell, A.K. Cheetham, D.E. Cox, J.S. Gardner, K. Hanit, A. dos Santos, and G.F. Strouse, *Phys. Rev. B* **61**, 15 269 (2000).
- <sup>23</sup>P. Carra and T.B. Thole, *Rev. Mod. Phys.* **66**, 1509 (1994).
- <sup>24</sup>The computer program can be freely downloaded at the address <http://www-cristallo.grenoble.cnrs.fr/simulation>
- <sup>25</sup>T.A. Tyson, K.O. Hodgson, C.R. Natoli, and M. Benfatto, *Phys. Rev. B* **46**, 5997 (1992).
- <sup>26</sup>Y. Joly, *Phys. Rev. B* **63**, 125120 (2001).
- <sup>27</sup>L. Hedin and B.I. Lundqvist, *J. Phys. C* **4**, 2064 (1971).
- <sup>28</sup>T. Chatterji, A. Stunault, J.A. Paixao, R. Suryanarayanan, G. Dhalenne, and A. Revcolevschi (unpublished).
- <sup>29</sup>S. Di Matteo and C.R. Natoli, *J. Synchrotron Radiat.* **9**, 9 (2002).